Sensors and Actuators B 213 (2015) 155–163

Contents lists available at ScienceDirect

Sensors and Actuators B: Chemical

journal homepage: www.elsevier.com/locate/snb

Synthesis of Zn_2SnO_4 via a co-precipitation method and its gas-sensing property toward ethanol

Dongmin An*, Qiong Wang, Xiaoqiang Tong, Qingjun Zhou, Zepeng Li, Yunling Zou, Xiaoxue Lian, Yan Li

College of Science, Civil Aviation University of China, Tianjin 300300, PR China

ARTICLE INFO

Article history:
Received 16 July 2014
Received in revised form 10 February 2015
Accepted 11 February 2015
Available online 19 February 2015

Keywords:
Zn_2SnO_4
Gas-sensing property
Ethanol

ABSTRACT

In this work, uniform Zn_2SnO_4 nanoparticles were synthesized with a simple co-precipitation method followed by hydrothermal post-treatment process. For comparison, pure ZnO and SnO_2 samples were obtained with the same method. These products were characterized by X-ray diffraction (XRD), field-emission scanning electron microscopy (FESEM), and N_2 absorption–desorption analysis. The ethanol-sensing properties of as-prepared Zn_2SnO_4 nanostructure sensor was systematically investigated and compared with the pure ZnO and SnO_2 sensors. The results revealed that the Zn_2SnO_4-based sensor exhibited a low operating temperature, high response, good repeatability, and long-term stability toward ethanol gas.

1. Introduction

With the increasing air pollution and the increased awareness of the influence of air quality to people's health, researchers have paid much attention to the air quality monitor and control, toxic or flammable gases detection, and medical diagnosis [1,2]. Gas sensor is a widely used material in the field of gas detection. Ethanol, a kind of volatile organic compounds, has been widely used in the chemical, biomedical, food industries, etc., especially in wine quality monitoring and analyzer. Because of its easy volatility and inflammability, the development of sensors with high selectivity, sensitivity and stability to detect ethanol gas in time is very important. To date, numerous semiconductor oxides, such as ZnO, SnO_2, WO_3 and Co_3O_4 [3–6], or their composites, such as ZnO–CuO, SnO_2–PbO, SnO_2–Fe_2O_3, ZnO–SnO_2, and C–SnO_2 [7–10], have been studied for ethanol detection. Moreover, great efforts have made to improve the properties of these gas sensors, including the sensitivity, stability, selectivity, and response–recovery speed, by means of preparing novel structure materials, or loading some noble metals to prepare composites [11–14].

Zn_2SnO_4, an n-type transparent ternary semiconductor with a band gap of 3.6 eV, has high electrical conductivity, high electron mobility, and attractive optical properties. Because of its excellent properties, it has been utilized in various areas, such as used as a photocatalyst for degradation of some organic pollutants in aqueous solution [15], anode material for Li-ion batteries, sensors for combustible gases [16–18], especially in the application of gas sensor to detect ethanol gas in the recent years. Zn_2SnO_4 with cubic and quasi-cubic morphologies had been synthesized by Jiang et al. [19] via a low temperature hydrothermal method and used as sensors to detect alcohol gas. Studies showed that the sensitivity (Ra/Rg) of Zn_2SnO_4 cuboctahedra reached 94.3 at alcohol concentration of 600 ppm under the optimum working temperature (325 °C) of Zn_2SnO_4 samples. Zn_2SnO_4 nanowires were prepared by Tharsika et al. [20], and the response of the Zn_2SnO_4 nanowires sensor to 50 ppm ethanol was about 21.6 at the optimum operating temperature of 500 °C. Chen et al. [21] had reported that Zn_2SnO_4 with flowerlike superstructures assembled with nanorods was highly sensitive to ethanol at 128 °C (Ra/Rg = 18, 50 ppm) after calcination. However, the results are not very satisfactory for the high operating temperature, or a low response to ethanol gas at relative low temperature.

Zn_2SnO_4 can be obtained by different routes such as hydrothermal method, traditional solid-state reaction, chemical vapor deposition, co-precipitation method [22–25], and so on. In this paper, Zn_2SnO_4 nanoparticles were synthesized by a simple co-precipitation method with a hydrothermal post-treatment, and their gas-sensing properties toward ethanol gas and other gases were discussed in detail. For comparison, pure ZnO and SnO_2 synthesized with the same method were also used as sensors to detect

* Corresponding author. Tel.: +86 22 2409 2624; fax: +86 22 2409 2514.
E-mail address: dman@cauc.edu.cn (D. An).

http://dx.doi.org/10.1016/j.snb.2015.02.042
0925-4005/

ethanol gas. The results indicated that the Zn_2SnO_4-based sensor presented an excellent gas-sensing property toward ethanol gas at low operating temperature.

2. Experimental procedures

2.1. Materials

Zinc acetate dihydrate ($Zn(CH_3COO)_2{\cdot}2H_2O$), ammonia ($NH_3{\cdot}H_2O$, 25%), tin tetrachloride ($SnCl_4{\cdot}5H_2O$), hexadecyltrimethylammonium bromide (CTAB), and ethanol (99.7%) of analytical grade were all used as received from Guo Yao Co., China.

2.2. Synthesis

In a typical synthesis procedures, 5 mmol CTAB was dissolved into a mixed solution of 25 mL of 0.1 M zinc acetate and 25 mL of 0.1 M tin tetrachloride with vigorous magnetic stirring at room temperature, then the ammonia aqueous solution (25% $NH_3{\cdot}H_2O$:H_2O = 2:11, volume ratio) was dropped into the above mixed solution at a rate of 0.5 mL/min with continued magnetic stirring until the pH of the mixed solution reached 7.0–8.0. The obtained white slurry was then transferred into a 100 mL Teflon stainless steel autoclave and the sealed autoclave was maintained at 120 °C for 24 h in an oven. Afterward the autoclave was cooled naturally to room temperature. The obtained slurry was filtrated, washed with water and absolute ethanol for several times, and dried at 80 °C for 12 h to obtain the white product. Subsequently, the white product was calcined in air at 500 °C for 3 h to get the final Zn_2SnO_4 product. The SnO_2 and ZnO samples were obtained by changing the material to 0.1 M $SnCl_4$ solution and 0.1 M zinc acetate solution, respectively, when other conditions were kept the same.

2.3. Sensor fabrication and measurements

The gas sensors were fabricated as described in our previous study [26]. Briefly, a small amount of as-obtained product was first ground with distilled water to form homogeneous slurry, then the slurry was coated onto a ceramic tube (4 mm in length and 1 mm in diameter) with a pair of gold electrodes and four platinum wires on both ends to form a thin film structure. A Ni–Cr alloy coil crossing the tube was used as a heater to control the operating temperature by tuning the heating current. The gas sensors were first aged at 300 °C for several hours before the gas-sensing properties were measured. The gas-sensing properties were tested in a chamber and target gas was first diluted with air and then was introduced into the test chamber by a microsyringe. The sensor response is defined as $S = Ra/Rg$, where Ra and Rg are the resistances of the ZnO sensor in air and in tested gas, respectively.

2.4. Characterizations

The obtained samples were characterized by powder X-ray diffraction (XRD) (DX-2000 X-ray diffractometer instrument with Cu K_α radiation, $\lambda = 0.15418$ nm). The microstructures of samples were observed by a field-emission-scanning electron microscope (FE-SEM, LEO1530VP). N_2 adsorption–desorption isotherms were analyzed by an ASAP 2020 instrument at 77 K. Chemical Gas Sensor-8 (CGS-8) intelligent gas sensing analysis system (Ailite Technology Co., Ltd., Beijing, China) was used to do the gas-sensing tests at a relative humidity (RH) of 25%.

3. Results and discussion

XRD was used to investigate the phase structure of as-synthesized calcined samples. According to the XRD patterns in Fig. 1a, the diffraction peaks of ZnO product could be indexed as the hexagonal wurtzite structure of ZnO, which were in good agreement with the standard JCPDS Card of ZnO (No. 36-1451). Moreover, the XRD diffraction peaks were rather broad indicating the nanocrystalline nature of the ZnO product. The diffraction peaks of SnO_2 sample were well in agreement with those of standard patterns of tetragonal cassiterite structure of SnO_2 (JPCDS file No. 21-1250) and the peaks were broad and weak, revealing a small crystal size of this sample. The diffraction peaks of the calcined Zn_2SnO_4 sample in Fig. 1a were more broad and weak, and well indexed to cubic spinel-structured Zn_2SnO_4 (JCPDS Card No. 74-2184). Additionally, no other impurity peaks were observed in the XRD patterns of the calcined Zn_2SnO_4 product, implying the inexistence of other impurities. Fig. 1b shows the XRD patterns of the as-synthesized Zn_2SnO_4 products before and after calcination. As can be seen, all the diffraction peaks of Zn_2SnO_4 products before and after calcination were coincident which indicated the Zn_2SnO_4 product was obtained in the solution process. The peak intensity of $2\theta = 34.3^\circ$ was strengthened after calcination process which was possibly due to better crystallinity of the calcined Zn_2SnO_4 sample. The Scherrer formula ($D = k\lambda/\beta\cos\theta$) is used to estimate the average grain size of calcined Zn_2SnO_4 sample, where D is the average grain size, k is the Scherrer constant (0.89), λ stands for the wavelength of X-ray, β is the peak width at half-maximum intensity, and θ is the diffraction angle. The calculated average grain size from this equation for the calcined Zn_2SnO_4 sample was 14 nm.

The reaction for formation of Zn_2SnO_4 can be summarized as follows:

$$NH_3H_2O \rightarrow NH_4^+ + OH^- \quad (1)$$

$$Zn^{2+} + Sn^{4+} + 6OH^- \rightarrow ZnSn(OH)_6\downarrow \quad (2)$$

$$Zn^{2+} + 4OH^- \rightarrow Zn(OH)_4^{2-} \quad (3)$$

$$Zn(OH)_4^{2-} + ZnSn(OH)_6 \rightarrow Zn_2SnO_4\downarrow + 4H_2O + 2OH^- \quad (4)$$

Fig. 2 depicts the SEM images of calcined ZnO, SnO_2, and Zn_2SnO_4 samples. As can be seen in Fig. 2a, the ZnO nanoparticles were spherical with some agglomeration and the average size of ZnO nanoparticles was about 20 nm, which was agreed with the XRD results. The calcined SnO_2 product in Fig. 2b showed an irregular morphology. Some particles were small nanospheres and some were large aggregates piled up with irregular SnO_2 nanoparticles. The calcined Zn_2SnO_4 sample in Fig. 2c showed the similar shape with the ZnO product, which were irregular spheres less than 20 nm, a little smaller than the size of ZnO nanoparticles.

The N_2 adsorption–desorption isotherms and pore size distribution curve of the calcined Zn_2SnO_4 sample are shown in Fig. 3. It can be seen in Fig. 3a, the isotherm of the Zn_2SnO_4 sample exhibited a type IV isotherm with a distinct H_2 hysteresis loop in the range of 0.4–0.8 P/P_0, which is typical of mesoporous materials according to the IUPAC classification. The hysteresis loop indicated the slit-shaped pores of Zn_2SnO_4 sample and the BET specific surface area was up to 111.2 m^2/g. The pore size distribution, which was calculated from the desorption branch of N_2 isotherm, is shown in Fig. 3b. A narrow peak of pore size distribution was centered at 3 nm, further confirming the mesoporous nature of this sample. The BET specific surface areas were calculated to be 48 m^2/g for ZnO and 11.1 m^2/g for SnO_2 samples, respectively, which was much lower than that of Zn_2SnO_4 and was consisted with SEM analysis. The results implied that the Zn_2SnO_4 product would exhibit more excellent activity in gas-sensing property.

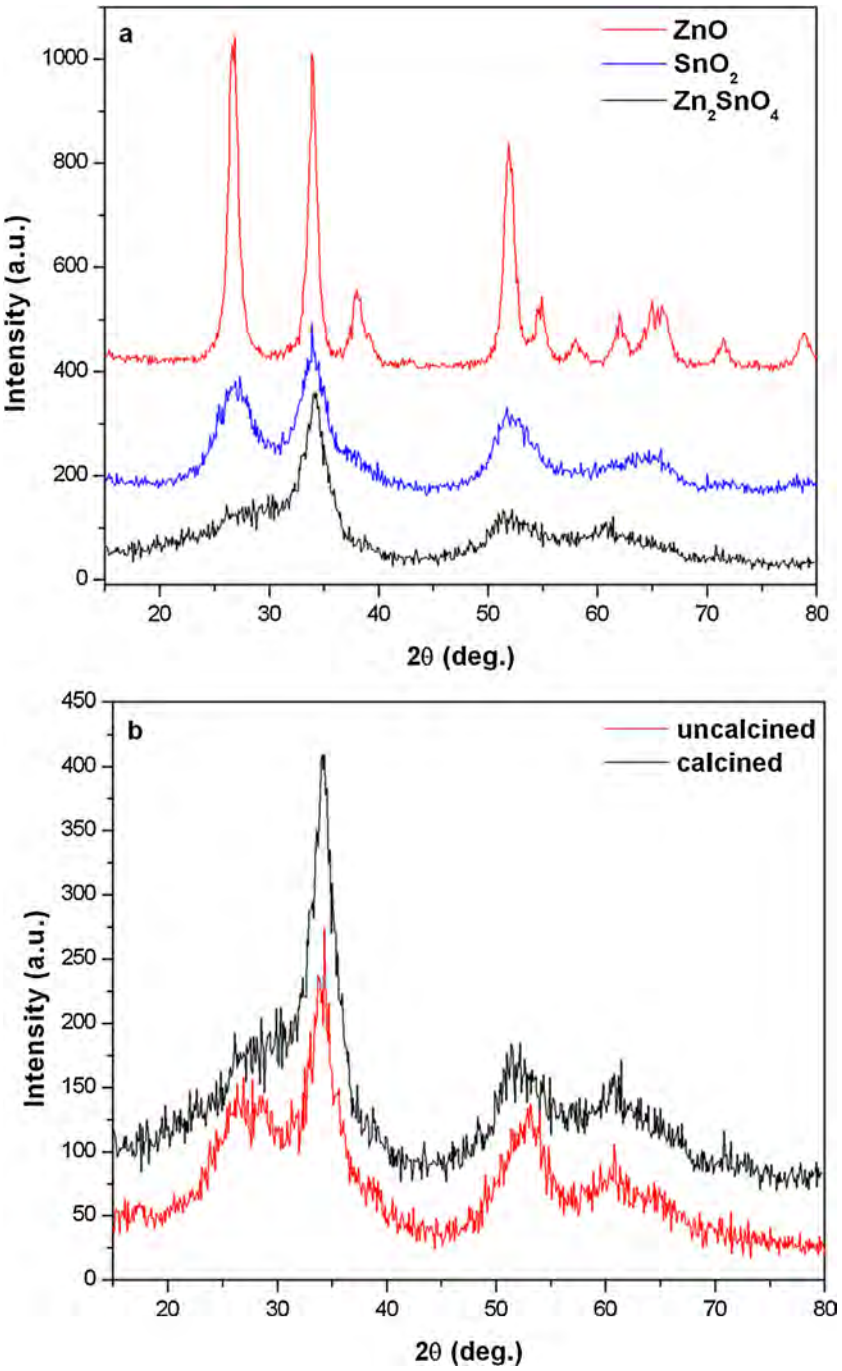

Fig. 1. The XRD of the obtained calcined pure ZnO, SnO_2 and Zn_2SnO_4 samples (a); the uncalcined Zn_2SnO_4 and calcined Zn_2SnO_4 samples (b).

A sensor based on the calcined Zn_2SnO_4 sample was fabricated. For comparison, the gas-sensing properties of the synthesized pure ZnO and SnO_2 samples were also studied. The relationship between the response and the operating temperature of these sensors was first investigated. As shown in Fig. 4, the responses of these sensors exposed to 50 ppm ethanol gas as a function of the operating temperature were displayed. If the operating temperature was too low, the chemical reaction was low, leading to a low response. With the increment of operating temperature, the response of Zn_2SnO_4 sensor first greatly increased in the range of 120–180 °C and reached the maximal value at 180 °C. After that, the response gradually decreased in the range of 180–300 °C. If the operating temperature was too high, the activity of ethanol gas molecules was high, resulting in the adsorbed gas molecules escaped from the surface of sensor easily before reactions taking place so as to a poor response as well. In addition, it could be clearly observed that the response of Zn_2SnO_4 sensor was superior to that of ZnO and SnO_2 sensors. The Zn_2SnO_4 sensor was highly sensitive to ethanol gas at the temperature of 180 °C, which was lower than that of ZnO (200 °C) and SnO_2 (240 °C) sensors. Furthermore, the response of Zn_2SnO_4 sensor to 50 ppm ethanol gas reached 26.5 at 180 °C that was much larger than that of ZnO (18.6, 200 °C) and SnO_2 (15.3, 240 °C) sensors. Therefore, the temperature of 180 °C was chosen for our further study on the gas-sensing properties of the as-prepared Zn_2SnO_4 sample. The optimum operating temperature was much lower and the response was higher than those reported Zn_2SnO_4

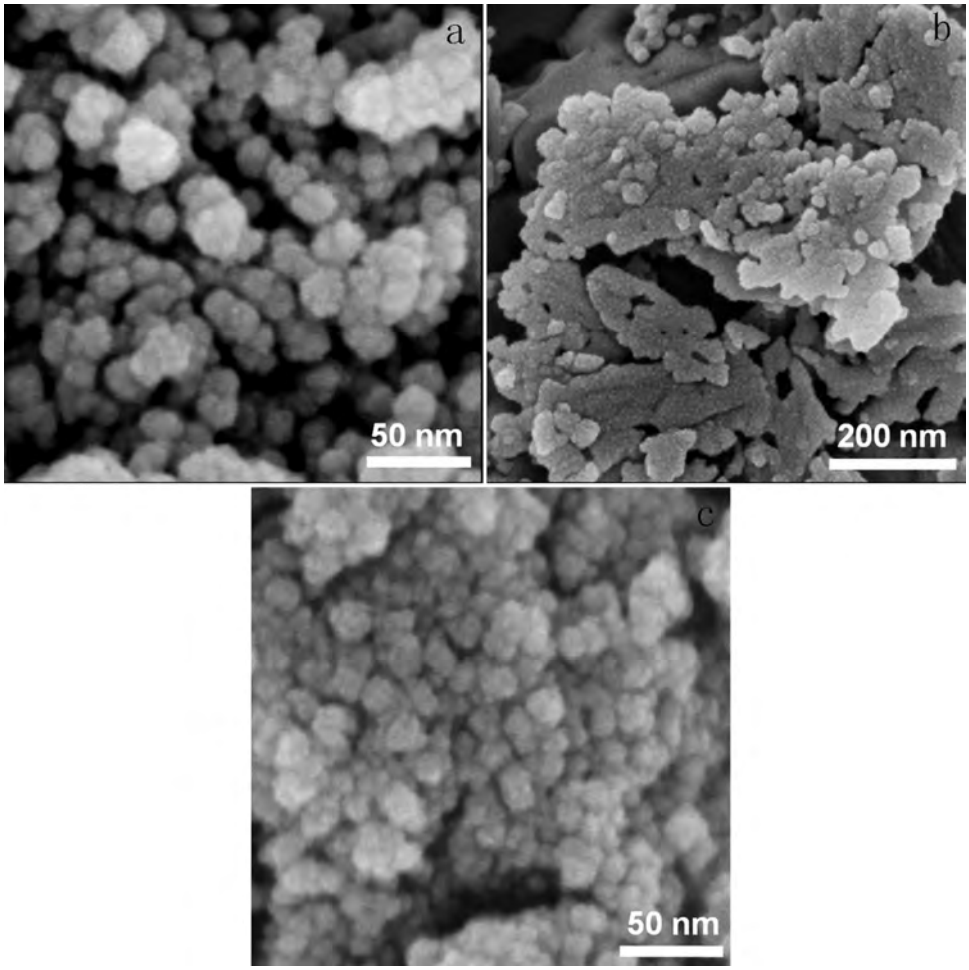

Fig. 2. The SEM images of the calcined ZnO (a), SnO_2 (b), and Zn_2SnO_4 products.

sensors [19,20] and other binary metal oxide based ethanol sensors [27–29].

Fig. 5 shows the gas-sensing properties of the Zn_2SnO_4, ZnO and SnO_2-based sensors toward different concentrations of ethanol gas at the optimal operating temperature. It displayed that the responses of ZnO, SnO_2 and Zn_2SnO_4 sensors increased with the increasing of ethanol concentration from 5 ppm to 200 ppm, and the response of Zn_2SnO_4 sensor was much better than that of ZnO and SnO_2 sensors. Among them, the responses of Zn_2SnO_4 sensor to ethanol gas between 5 and 100 ppm increased the most quickly. To 100 ppm ethanol gas, the response of Zn_2SnO_4 sensor was up to 46.5 while the response values were only 22.5 and 21.6 for ZnO and SnO_2 sensors, respectively. With the ethanol concentration further increasing, the response of Zn_2SnO_4 sensor became increased slowly. The result implied that the Zn_2SnO_4 sample was promising to detect low concentration of ethanol gas.

Fig. 6a shows the dynamic response–recovery curves of the Zn_2SnO_4 sensor to ethanol gas from 5 ppm to 100 ppm at 180 °C. It was obvious that with the increment of ethanol gas concentration, the response increased. Not only to the high ethanol gas concentration, but also to a low concentration of 5 ppm ethanol gas, the Zn_2SnO_4 sensor gave a considerable response. The gas-sensing property of the same Zn_2SnO_4 sensor was repeatedly examined 20 days later, as shown in Fig. 6a, the response of the sensor was nearly weaken when it was exposed to 5–100 ppm ethanol gas at 180 °C after 20 days, which implied the stability and reproducibility performances of the Zn_2SnO_4 sensor. The repeatability and long-time stability of the Zn_2SnO_4 sensor were further investigated by applying the sensor to successive gas-sensing test in five cycles to 5 ppm ethanol gas at 180 °C over a period of 20 days. As shown in Fig. 6b, the Zn_2SnO_4-based sensor was exposed to ethanol gas and air dynamically. It could be observed that the response and recovery characteristics were repeatable when the gas control switch was set between on and off, revealing an excellent repeatability and long-term stability of the sensor. Furthermore, in our experiment, the Zn_2SnO_4-based sensor also had good responses to other testing gases as shown in Fig. 6c. It can be found that the Zn_2SnO_4 sensor exhibited a considerable response to 50 ppm of CH_3COCH_3 (15), C_6H_6 (12.7), CO (14), and CH_4 (13.1) gas at 180 °C, respectively, which was superior to the results reported in the literatures [30,31]. It indicated that the Zn_2SnO_4 nanoparticles were highly promising for applications of gas sensors.

Other reports [32–34] had demonstrated that the gas-sensing properties of a semiconductor metal oxide were also affected by the testing humidity. The Zn_2SnO_4-based sensor was investigated to detect 50 ppm ethanol gas under different relative humidities. As shown in Fig. 7, the response of the sensor was obviously influenced by the relative humidity and showed a large decrease from 26.5 to 13.6 with the increment of relative humidity from 25% to 70%. Generally, the higher the testing humidity was, the more immeasurable chemisorption/physisorption of water molecules were absorbed on the surface of sensor [32,33], which might interfere with the sensing reactions by replacing the oxygen species preadsorbed on

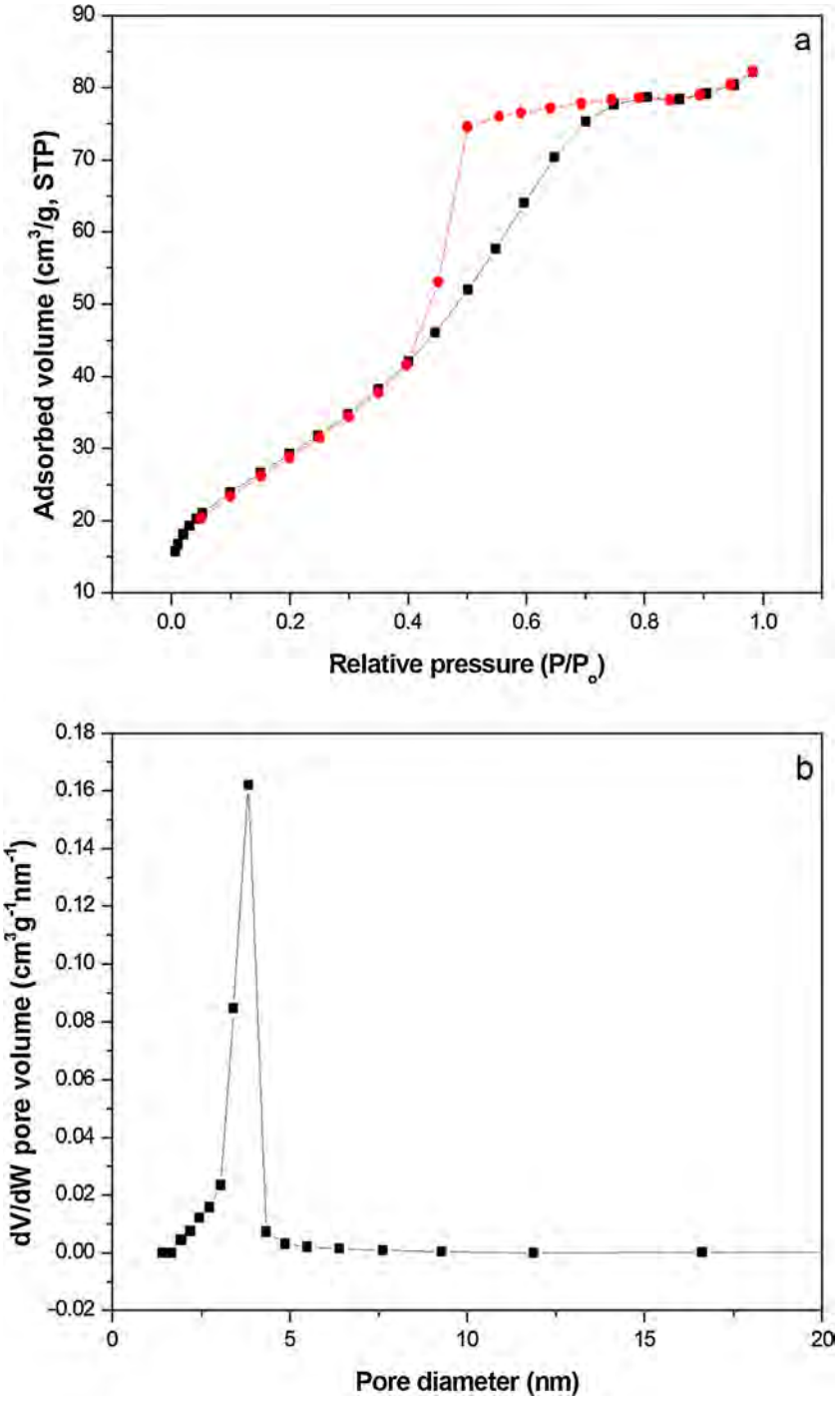

Fig. 3. The curves of nitrogen adsorption–desorption isotherms (a) and pore size distribution of calcined Zn_2SnO_4 nanoparticles (b).

the surface of Zn_2SnO_4. Moreover, the relative high specific surface area of the obtained Zn_2SnO_4 material also affected the chemisorption/physisorption of water molecules absorbed on the surface of the sensor. These factors led to the activity of the sensing layer of gas sensors decreased, and hence decreased the response to the ethanol gas.

The dynamic response–recovery curves of the ZnO, SnO_2, and Zn_2SnO_4 sensors to 5 ppm ethanol gas are shown in Fig. 8. When the ethanol gas was introduced, the response increased with time, all the samples needed only several seconds to reach the maximum values of the respond. Besides, for the ZnO and SnO_2 sensors, they also had a very short recovery time to return to its initial value when the sensors were exposed to the atmospheric air; while for the Zn_2SnO_4 sensor, more time was needed to recovery. That may due to its small crystalline size and the large surface area. Generally, small particle size will lead to the specific surface area higher. Large surface area could lead more oxygen molecules absorbed on the surface of the Zn_2SnO_4 particles in the air, and more free electrons from the conduction band to form chemisorbed oxygen species (O^{2-}, O_2^{2-}, and O^-) were captured. When the Zn_2SnO_4 sensor was exposed to ethanol or other reductive gases, the adsorbed oxygen species on the surface reacted with these gas molecules, leading to a decrease in the resistance of an n-type semiconductor. Therefore, the specific surface area of the Zn_2SnO_4

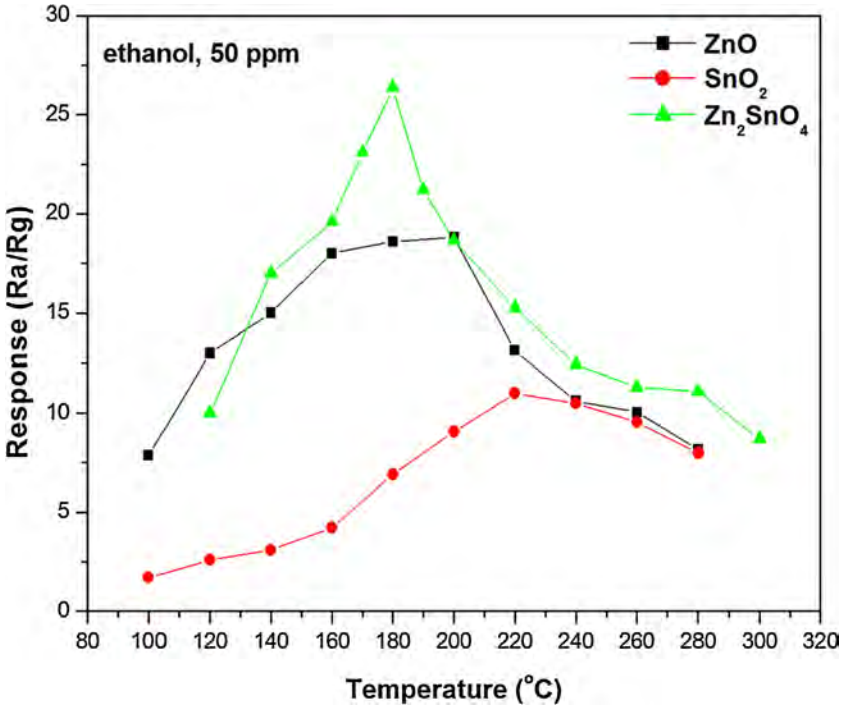

Fig. 4. Response of the calcined ZnO, SnO_2, and Zn_2SnO_4-based sensors to 50 ppm ethanol gas at different working temperatures.

particles played an important role in the contact and subsequent reaction of oxygen species with the tested gas. The surface area of Zn_2SnO_4 sample was up to 111.2 m^2/g, which was much higher than that of the Zn_2SnO_4 products in references [16,19]. In our case, we believed that the high responses of the Zn_2SnO_4 sensor to ethanol and other gases could be ascribed to the smaller crystallize size and larger specific surface area of the sensing materials.

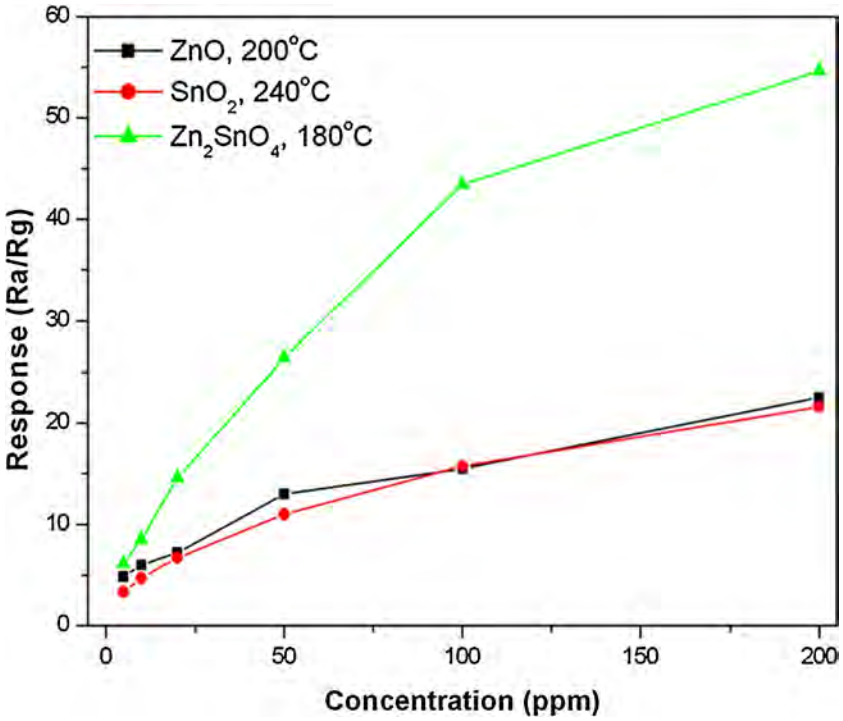

Fig. 5. Response of the calcined ZnO, SnO_2, and Zn_2SnO_4-based sensors versus ethanol gas concentrations from 5 to 200 ppm.

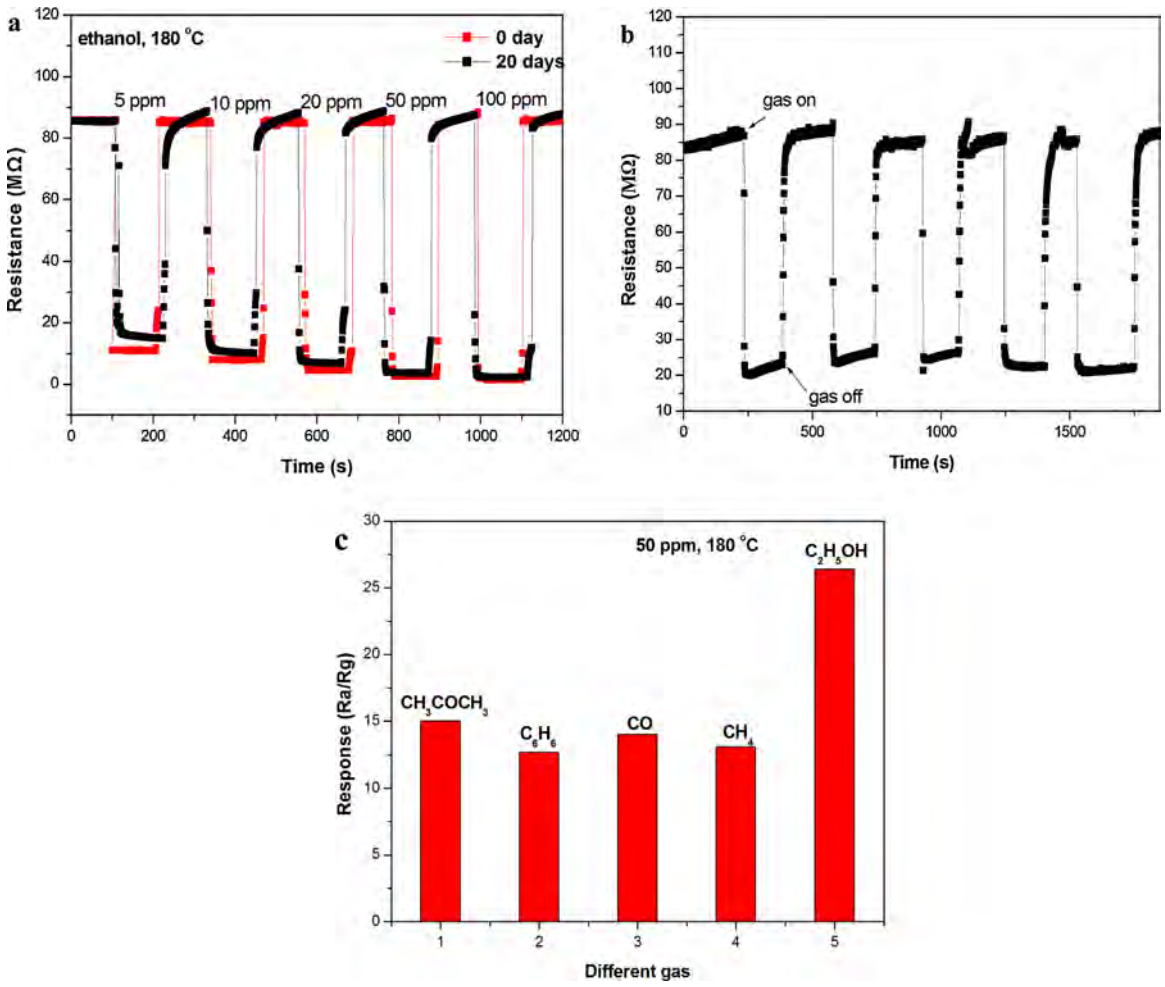

Fig. 6. Response–recovery curves of the calcined Zn_2SnO_4 sensor to different concentrations of ethanol gas at 180 °C (a); The repeatability and long-term stability of the calcined Zn_2SnO_4 sensor to 5 ppm of ethanol gas (b); and the responses of the calcined Zn_2SnO_4 sensor to 50 ppm different testing gases (c).

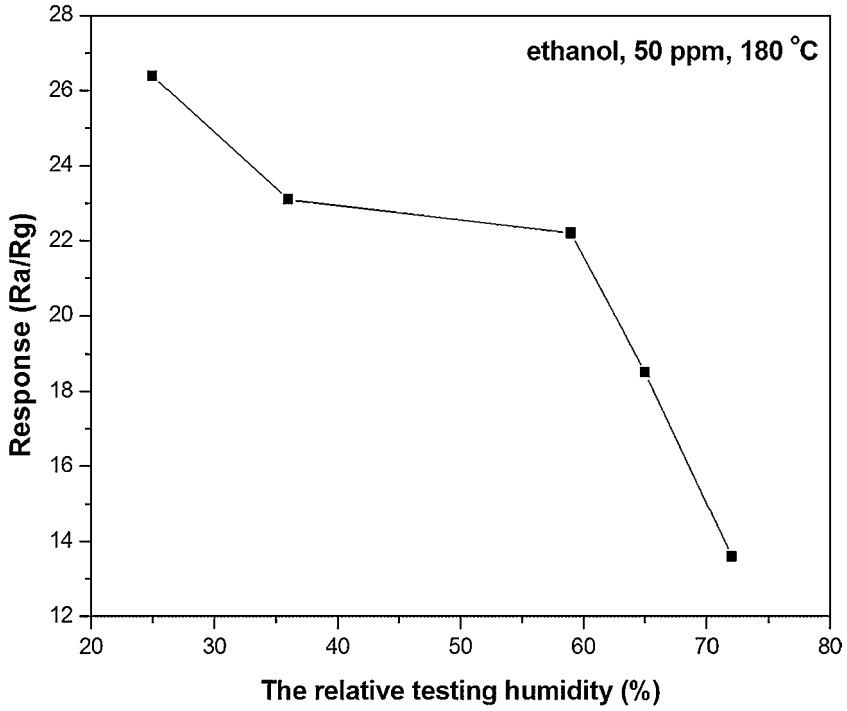

Fig. 7. Response of the calcined Zn_2SnO_4 sensor to 50 ppm of ethanol gas at different relative humidities.

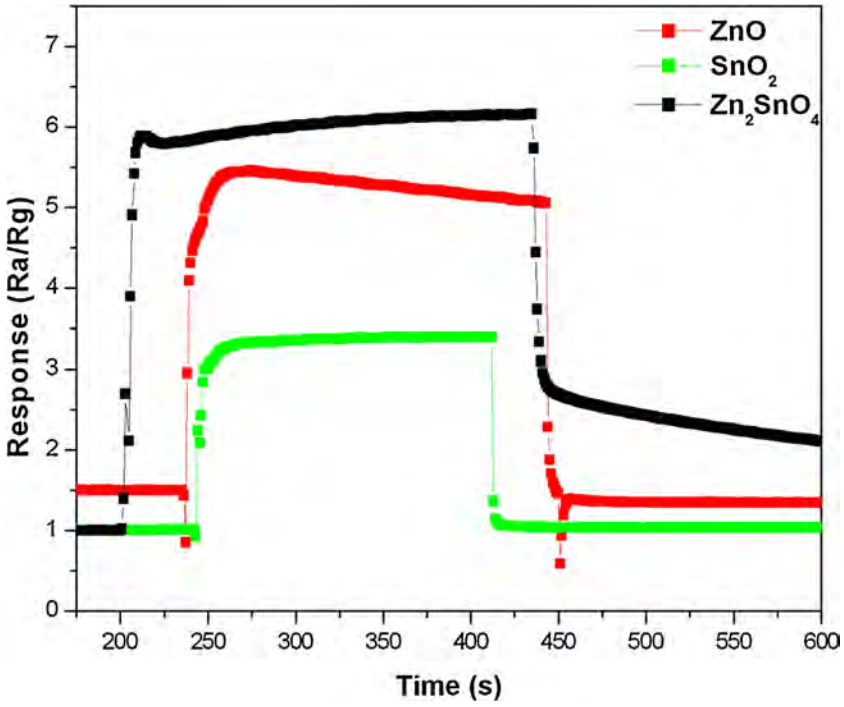

Fig. 8. Response–recovery curves of the calcined ZnO (200 °C), SnO_2 (240 °C), and Zn_2SnO_4 (180 °C) to 5 ppm ethanol gas, respectively.

4. Conclusions

In summary, uniform Zn_2SnO_4 nanoparticles (about 20 nm) were facilely synthesized, which characterized a larger surface area and narrow pore size distribution than pure ZnO and SnO_2 powders obtained with the same method. Among ethanol gas-sensing examinations of as-synthesized compounds, Zn_2SnO_4 showed lower operating temperature (180 °C) than ZnO, SnO_2 and Zn_2SnO_4 reported elsewhere in conditions of 50 ppm ethanol gas. At respective optimum operating temperature, the responses of as-synthesized Zn_2SnO_4 to 100 ppm ethanol gases was approximately 2 fold increase as compared with as-synthesized ZnO, SnO_2. Besides, as-synthesized Zn_2SnO_4 showed an excellent repeatability, and long-term stability to ethanol gas. All these excellent gas-sensing properties make this material have a broad application foreground in detection of ethanol gas.

Acknowledgements

The project was mainly supported by the Fundamental Research Funds for the Central Universities (ZXH2012K008, 3122013D008 and 3122013k007), the Significant Pre-research Funds of Civil Aviation University of China (No. 3122013P001), the Science and Technology Innovation Guide Funds of Civil Aviation Administration of China (2014), is supplemented as (MHRD20140209) and the Applied Basic and Cutting-edge Research Programs of Science and Technology Foundation of Tianjin (No. 13JCQNJC07100).

References

[1] V.V. Sysoev, B.K. Button, K. Wepsiec, S. Dmitriev, A. Kolmakov, Toward the nanoscopic "electronic nose": hydrogen vs carbon monoxide discrimination with an array of individual metal oxide nano- and mesowire sensors, Nano Lett. 6 (2006) 1584–1588.
[2] F. Sun, W. Cai, Y. Li, L. Jia, F. Lu, Direct growth of mono- and multilayer nanostructured porous films on curved surfaces and their application as gas sensors, Adv. Mater. 17 (2005) 2872–2877.
[3] L.W. Wang, Y.F. Kang, X.H. Liu, S.M. Zhang, W.P. Huang, S.R. Wang, ZnO nanorod gas sensor for ethanol detection, Sens. Actuators B 162 (2012) 237–243.
[4] Y. Zhang, X.L. He, J.P. Li, Z.J. Miao, F. Huang, Fabrication and ethanol-sensing properties of micro gas sensor based on electrospun SnO_2 nanofibers, Sens. Actuators B 132 (2008) 67–73.
[5] Z. Wen, L.P. Zhu, Y.G. Li, Z.Y. Zhang, Z.Z. Ye, Mesoporous Co_3O_4 nanoneedle arrays for high-performance gas sensor, Sens. Actuators B 203 (2014) 873–879.
[6] R. Ionescu, A. Hoel, C.G. Granqvist, E. Llobet, P. Heszler, Low-level detection of ethanol and H_2S with temperature-modulated WO_3 nanoparticle gas sensors, Sens. Actuators B 104 (2005) 132–139.
[7] N.D. Khoang, D.D. Trung, N.V. Duy, N.D. Hoa, N.V. Hieu, Design of SnO_2/ZnO hierarchical nanostructures for enhanced ethanol gas-sensing performance, Sens. Actuators B 174 (2012) 594–601.
[8] Y.B. Zhang, J. Yin, L. Li, L.X. Zhang, L.J. Bie, Enhanced ethanol gas-sensing properties of flower-like p-CuO/n-ZnO heterojunction nanorods, Sens. Actuators B 202 (2014) 500–507.
[9] N.V. Hieu, N.A.P. Duc, T. Trung, M.A. Tuan, N.D. Chien, Gas-sensing properties of tin oxide doped with metal oxides and carbon nanotubes: a competitive sensor for ethanol and liquid petroleum gas, Sens. Actuators B 144 (2010) 450–456.
[10] X.Y. Feng, J. Jiang, H. Ding, R.M. Ding, D. Luo, J.H. Zhu, Y.M. Feng, X.T. Huang, Carbon-assisted synthesis of mesoporous SnO_2 nanomaterial as highly sensitive ethanol gas sensor, Sens. Actuators B 183 (2013) 526–534.
[11] C.L. Hsu, Y.D. Gao, Y.S. Chen, T.J. Hsueh, Vertical Ti doped ZnO nanorods based on ethanol gas sensor prepared on glass by furnace system with hotwire assistance, Sens. Actuators B 192 (2014) 550–557.
[12] P. Sun, X. Zhou, C. Wang, B. Wang, X.M. Xu, G.Y. Lu, One-step synthesis and gas sensing properties of hierarchical Cd-doped SnO_2 nanostructures, Sens. Actuators B 190 (2014) 32–39.
[13] S.S. Tian, S.Y. Lou, S.M. Zhou, Monoclinic α-Ag_2S hollow nanospheres: promising candidates for ethanol gas sensors at room-temperature, Mater. Lett. 137 (2014) 382–384.
[14] J.F. Ding, X.M. Li, J. Cao, L.Y. Sheng, L.Z. Yin, X.M. Xu, New sensor for gases dissolved in transformer oil based on solid oxide fuel cell, Sens. Actuators B 202 (2014) 232–239.
[15] E.L. Feletto, J.M. Simões, M.A. Mazutti, et al., Application of Zn_2SnO_4 photocatalyst prepared by microwave-assisted hydrothermal route in the degradation of organic pollutant under sunlight, Ceram. Int. 39 (2013) 4569–4574.
[16] Z. Chen, M.H. Cao, C.W. Hu, Novel Zn_2SnO_4 hierarchical nanostructures and their gas sensing properties toward ethanol, J. Phys. Chem. C 115 (2011) 5522–5529.
[17] K. Wang, Y. Huang, T. Zh Han, Y. Zhao, H.J. Huang, L. Xue, Facile synthesis and performance of polypyrrole-coated hollow Zn_2SnO_4 boxes as anode materials for lithium-ion batteries, Ceram. Int. 40 (2014) 2359–2364.
[18] Y.Q. Jiang, C.X. He, R. Sun, Z.X. Xie, L.S. Zheng, Synthesis of Zn_2SnO_4 nanoplate-built hierarchical cube-like structures with enhanced gas-sensing property, Mater. Chem. Phys. 136 (2012) 698–704.
[19] Y.Q. Jiang, X.X. Chen, R. Sun, Z. Xiong, L.S. Zheng, Hydrothermal synthesis and gas sensing properties of cubic and quasi-cubic Zn_2SnO_4, Mater. Chem. Phys. 129 (2011) 53–61.
[20] T. Tharsika, A.S.M.A. Haseeb, S.A. Akbar, M.F.M. Sabri, Y.H. Wong, Gas sensing properties of zinc stannate (Zn_2SnO_4) nanowires prepared by carbon assisted thermal evaporation process, J. Alloys Compd. 618 (2015) 455–462.

[21] C. Chen, G.Z. Li, J.H. Li, Y.L. Liu, One-step synthesis of 3D flower-like Zn_2SnO_4 hierarchical nanostructures and their gas sensing properties, Ceram. Int. (2014), http://dx.doi.org/10.1016/j.ceramint.2014.09.136.
[22] Z.H. Ai, S.C. Lee, Y. Huang, W.K. Ho, L.Z. Zhang, Photocatalytic removal of NO and HCHO over nanocrystalline Zn_2SnO_4 microcubes for indoor air purification, J. Hazard. Mater. 179 (2010) 141–150.
[23] B. Tan, E. Toman, Y.G. Li, Y.Y. Wu, Zinc stannate (Zn_2SnO_4) dye-sensitized solar cells, J. Am. Chem. Soc. 129 (2007) 4162–4163.
[24] H.F. Lin, S.C. Liao, S.W. Hung, C.T. Hu, Thermal plasma synthesis and optical properties of Zn_2SnO_4 nanopowders, Mater. Chem. Phys. 117 (2009) 9–13.
[25] T. Lim, H. Kim, M. Meyyappan, S. Ju, Photostable Zn_2SnO_4 nanowire transistors for transparent displays, ACS Nano 6 (2012) 4912–4920.
[26] D.M. An, Y. Li, X.X. Lian, Y.L. Zou, G.Z. Deng, Synthesis of porous ZnO structure for gas sensor and photocatalytic applications, Colloids Surf. A: Physicochem. Eng. Asp. 447 (2014) 81–87.
[27] X.Q. Wang, M.F. Zhang, J.Y. Liu, T. Luo, Y.T. Qian, Shape- and phase-controlled synthesis of In_2O_3 with various morphologies and their gas-sensing properties, Sens. Actuators B 137 (2009) 103–110.
[28] F.H. Zhang, H.Q. Yang, X.L. Xie, L. Li, L.H. Zhang, J. Yu, H. Zhao, B. Liu, Controlled synthesis and gas-sensing properties of hollow sea urchin-like α-Fe_2O_3 nanostructures and α-Fe_2O_3 nanocubes, Sens. Actuators B 141 (2009) 381–389.
[29] S. Singh, H. Kaur, V.N. Singh, K. Jain, T.D. Senguttuvan, Highly sensitive and pulse-like response toward ethanol of Nb doped TiO_2 nanorods based gas sensors, Sens. Actuators B 171–172 (2012) 899–906.
[30] B. Wang, Z.Q. Zheng, L.F. Zhu, Y.H. Yang, H.Y. Wu, Self-assembled and Pd decorated Zn_2SnO_4/ZnO wire-sheet shape nano-heterostructures networks hydrogen gas sensor, Sens. Actuators B 195 (2014) 549–561.
[31] H. Chen, Q.W. Wang, C.L. Kou, Y.M. Sui, Y. Zeng, F. Du, One-pot synthesis and improved sensing properties of hierarchical flowerlike SnO_2 assembled from sheet and ultra-thin rod subunits, Sens. Actuators B 194 (2014) 447–453.
[32] Q. Kuang, C.S. Lao, Z.L. Wang, Z.X. Xie, L.S. Zheng, High-sensitivity humidity sensor based on a single SnO_2 nanowire, J. Am. Chem. Soc. 129 (2007) 6070–6071.
[33] N. Yamazoe, Y. Shimizu, Humidity sensors: principles and applications, Sens. Actuators 10 (1986) 379–398.
[34] J. Zhang, J. Guo, H.Y. Xu, B.Q. Cao, Reactive-template fabrication of porous SnO_2 nanotubes and their remarkable gas-sensing performance, ACS Appl. Mater. Interfaces 5 (2013) 7893–7898.

Biographies

Dongmin An was born in Heibei, China, in 1983. She received her B.S. degree from the Changchun Institute of Technology of China in 2006 and then worked as a graduate student for five years at Jilin University, and received her doctor's degree in 2011 in China. Now, she worked at College of Science of Civil Aviation University of China in Tianjin as a lecturer. Her research interests include the synthesis of some functional nanomaterials, metal oxide semiconductor material, novel materials for photocatalysis and gas sensor, and so on.

Qiong Wang received his B.S. degree in 2007 and Ph.D. degree in 2012 in physical chemistry from the College of Chemistry and Chemical Engineering, Lanzhou University, China. He is currently a lecturer in College of Science of Civil Aviation University of China in Tianjin. His research interest is gas sensors based on semiconducting functional materials.

Xiaoqiang Tong is a lecturer at Civil Aviation University of China in Tianjin, he received Ph.D. from Jilin University in 2012, followed by postdoc at State Key Laboratory on Integrated Optoelectronics, Jilin University. His research interests includes inorganic nanoporous materials, functional inorganic coatings/films.

Qingjun Zhou is an associate professor at Civil Aviation University of China in Tianjin, he received Ph.D. from Jilin University in 2009. His research interests are in thearea of new materials for use inSolid Oxide Fuel Cells.

Zepeng Li received his B.S. from Ludong University of China in 2004 and then worked as a graduate student at Jilin University and received his M.S. and Ph.D. in 2007 and 2010 in China. Now, he worked at Civil Aviation University of China in Tianjin as a lecturer. His research interests includethe synthesis of semiconductor nanomaterials and pressure induced structure and properties changes of nanomaterials, and so on.

Yunling Zou received her MSc degree in Chemistry in 2006 from Liaoning Normal University, China. Since 2006 she has been working as an experimentalist at Civil Aviation University of China. Her research interests concern optical and morphological investigations on metal oxide nanomaterials. From 2012 to now she has been working on her doctor degree in Chemical Engineering in Tianjin University. Her Ph.D. research activities had been focused on the chemical synthesis of TiO_2 nanocrystals by means of chemical techniques and their applications in photocatalysis.

Xiaoxue Lian received her bachelor degree in 2012 at Civil AviationUniversity of China. At present, her research interest is focused on microstructure and gas sensing properties of semiconductor functional nanomaterials.

Yan Li completed his MS degree in mineral materials in 1997 and his Ph.D. in the field of nanomaterials in 2000 from Central South University. He was appointed as a full-time professor in Civil Aviation University of China in 2007. His research interests are functional materials, gas sensors, and mineral materials.